Contribution from the Department of Chemistry, University of Western Ontario, London, Ontario, Canada N6A 5B7, and Chemistry Division, National Research Council of Canada,† Ottawa, Ontario, Canada K1A 0R9

Electronic Structure of Square-Planar *cis*-Bis(trifluoromethyl)platinum(II) Complexes from UV Photoelectron Spectra and SCF-MS-Xα Calculations

Dong-Sheng Yang,‡ G. Michael Bancroft,*,‡ R. J. Puddephatt,*,‡ and John S. Tse§

Received May 5, 1989

UV photoelectron spectra of *cis*-$[Pt(CF_3)_2L_2]$ (L_2 = 1,5-cyclooctadiene (COD), $Me_2NCH_2CH_2NMe_2$ (TMED); L = PEt_3, $AsMe_3$) are reported, as well as MS-Xα calculations on the model compounds $[Pt(CF_3)_2(C_2H_4)_2]$ and *cis*-$[Pt(CF_3)_2(PH_3)_2]$. The spectra are assigned by using MS-Xα calculations and by comparison with the spectra of the corresponding dimethylplatinum(II) complexes. The first two ionization bands (with lowest ionization energies) are assigned to platinum-ligand σ orbitals, followed by four bands due to the essentially nonbonding platinum 5d orbitals. The nature of the Pt-CF_3 σ bonding is discussed in terms of MS-Xα results. In contrast to the Pt-CH_3 σ bonds, the Pt-CF_3 σ bonds have a significant C 2s and C-F antibonding character.

Introduction

It has long been recognized that perfluoroalkyl transition-metal complexes in general have properties very different from those of the corresponding alkyl complexes. For example, the perfluoroalkyl compounds have enhanced thermal stability[1,2] and shorter metal-carbon bond lengths compared to their alkyl analogues.[3,4] In platinum(II) complexes, perfluoroalkyl groups have a high NMR trans influence, comparable to that of the methyl group.[5,6] Replacement of methyl groups bound to platinum(II) by trifluoromethyl groups leads to deactivation of the metal center toward oxidative-addition reactions.[7,8] A ligand L is more readily displaced from *cis*-$[Pt(CF_3)_2L_2]$ than from *cis*-$[PtMe_2L_2]$.[8] Together these observations show that the platinum centers are more susceptible to nucleophilic attack but less susceptible to electrophilic attack when R = CF_3 rather than CH_3 in *cis*-$[PtR_2L_2]$ complexes. This is expected because of the greater electron-withdrawing power of CF_3 compared to CH_3.

The unusual effects of fluorine as a substituent are normally attributed to three of its special properties: (a) its high electronegativity, (b) the three nonbonding electron pairs on F, and (c) the good energy match between the F 2s and 2p orbitals and the corresponding orbitals of the carbon atom. On the basis of these properties, it was suggested that the unusual chemistry of the perfluoroalkyl transition-metal complexes was at least in part due to π back-bonding between filled d orbitals on the metal atom and σ^* orbitals of the perfluoroalkyl group.[1,9] Later, it was suggested that the π back-bonding was not important,[10] and Fenske and Hall concluded from their approximate molecular orbital calculations on $MeMn(CO)_5$ and $(CF_3)Mn(CO)_5$[11] that the significant differences between the alkyl and perfluoroalkyl complexes could be understood in terms of σ donation from an antibonding CF_3 orbital and energy stabilization due to the effects of charge on neighboring atoms. Since a detailed study of the electronic structure of square-planar *cis*-dimethylplatinum(II) complexes has been undertaken in our group,[12] a further investigation of the electronic structure of the corresponding perfluoromethyl complexes would be valuable to help to understand their differences in chemical properties and reactions.

In this paper, the UV photoelectron spectra of *cis*-$[Pt(CF_3)_2L_2]$ (L_2 = 1,5-cyclooctadiene (COD), $Me_2NCH_2CH_2NMe_2$ (TMED); L = PEt_3, $AsMe_3$) and MS-Xα calculations on the model compounds *cis*-$[Pt(CF_3)_2(C_2H_4)_2]$ and *cis*-$[Pt(CF_3)_2(PH_3)_2]$ are reported. The nature of the C-F bonding and the effect of the CF_3 groups on the MO energies and on the platinum bonding to the ligands L in these complexes are discussed.

Experimental Section

$[PtMe_2(COD)]$[12] was used as starting material for the preparation of $[Pt(CF_3)_2(COD)]$. $[PtMe_2(COD)]$ (1.30 g, 3.9 mmol) was placed in a 20-mL thick-walled Carius tube and dissolved in 1.5 mL of dichloromethane. The solution was frozen and degassed twice by using conventional freeze-thaw vacuum techniques. Trifluoromethyl iodide (11 mL) was condensed into the tube, and the Carius tube was sealed. The solution was warmed to room temperature and was allowed to stand for 5 days. The solution was filtered. The filtrate was passed through a Florisil column, eluting with dichloromethane, to give a orange-yellow solution first and then a very pale yellow solution. The volume of the pale yellow solution collected was reduced and *n*-pentane added to give white crystals. After the mixture was cooled at 0 °C for 1 h, the crystals of $[Pt(CF_3)_2(COD)]$ were filtered out and washed with a small amount of *n*-pentane: yield 0.83 g (48%); mp 179-181 °C. Other bis(trifluoromethyl)platinum(II) complexes were prepared by replacement of COD with the desired ligand L according to the literature method.[2] The compounds were sublimed prior to running the spectra, and their purity and identity were checked by melting points and NMR spectra. Spectral data for the new compound with L = PEt_3 (white, mp 141-143 °C) are as follows. ^{19}F NMR (CD_2Cl_2): δ -21.65 (^2J(Pt-F) = 617.3 Hz, Pt-CF_3; ^3J(P-F) = 65.8 Hz, CF_3-Pt-PEt_3). ^{31}P NMR (CD_2Cl_2): δ 17.58 (^1J(Pt-P) = 2840 Hz, Pt-PEt_3). Anal. For $C_{14}H_{30}F_6P_2Pt$. Calcd: C, 29.42; H, 5.67. Found: C, 29.51; H, 5.38.

UV photoelectron spectra were recorded on a McPherson ESCA-36 spectrometer equipped with a hallow-cathode UV He lamp[13] at temperatures within 30 °C of the melting point of each compound. The calibration and computer fitting of the spectra were performed as described before.[12]

The calculations presented here were performed by using the relativistic version of the Xα scattered-wave method,[14] in which the relativistic radial wave functions for the Pt atom have been employed. The exchange α parameters used in each atomic region were taken from the Schwarz tabulation[15] except for hydrogen, for which 0.777 25 was used.[16] For the extramolecular and intersphere regions, a weighted average of the

† NRCC Contribution No. 30029.
‡ University of Western Ontario.
§ National Research Council of Canada.

(1) King, R. B.; Bisnette, M. B. *J. Organomet. Chem.* **1964**, *2*, 15.
(2) Clark, H. C.; Manzer, L. E. *J. Organomet. Chem.* **1973**, *59*, 411.
(3) Churchill, M. R. *Inorg. Chem.* **1965**, *4*, 1734.
(4) Manojlovic-Muir, L.; Muir, K. W.; Solomun, T.; Meek, D. W.; Peterson, J. L. *J. Organomet. Chem.* **1978**, *146*, C26.
(5) Appleton, T. G.; Chisholm, M. H.; Clark, H. C.; Manzer, L. E. *Inorg. Chem.* **1972**, *11*, 1786.
(6) Appleton, T. G.; Bennett, M. A. *Inorg. Chem.* **1978**, *17*, 738. Bennett, M. A.; Chee, H.-K.; Roberston, G. B. *Inorg. Chem.* **1979**, *18*, 1061.
(7) Appleton, T. G.; Clark, H. C.; Manzer, L. E. *J. Organomet. Chem.* **1974**, *65*, 275.
(8) Appleton, T. G.; Hall, J. R.; Neale, D. W.; Williams, M. A. *J. Organomet. Chem.* **1984**, *276*, C73. Appleton, T. G.; Berry, R. D.; Hall, J. R.; Neale, D. W. *J. Organomet. Chem.* **1988**, *342*, 399.
(9) Cotton, F. A.; McCleverty, J. A. *J. Organomet. Chem.* **1964**, *2*, 15. Clark, H. C.; Tsai, J. H. *J. Organomet. Chem.* **1967**, *7*, 515.
(10) Graham, W. A. G. *Inorg. Chem.* **1968**, *7*, 315. Johnson, M. P. *Inorg. Chim. Acta* **1969**, *3*, 232.
(11) Hall, M. B.; Fenske, R. F. *Inorg. Chem.* **1972**, *11*, 768.
(12) Yang, D. S.; Bancroft, G. M.; Dignard-Bailey, L.; Puddephatt, R. J.; Tse, J. S. *Inorg. Chem.*, preceding paper in this issue.
(13) Bancroft, G. M.; Adams, J.; Coatsworth, L. L.; Bennewitx, C. D.; Brown, J. D.; Westwood, W. D. *Anal. Chem.* **1975**, *47*, 586.
(14) Johnson, K. H.; *Adv. Quantum Chem.* **1973**, *7*, 147. Herman, F.; William, A. R.; Johnson, K. H. *J. Chem. Phys.* **1974**, *61*, 3508. Case, D. A.; Yang, C. Y. *Int. J. Quantum Chem.* **1980**, *18*, 1091. Cook, M.; Case, D. A. *QCPE* **1982**, *14*, 465.
(15) Schwartz, K. *Phys. Rev. B.* **1972**, *5*, 2466. Schwartz, K. *Theor. Chim. Acta* **1974**, *34*, 225.
(16) Slater, J. C. *Int. J. Quantum Chem.* **1973**, *7s*, 533.

0020-1669/90/1329-2496$02.50/0

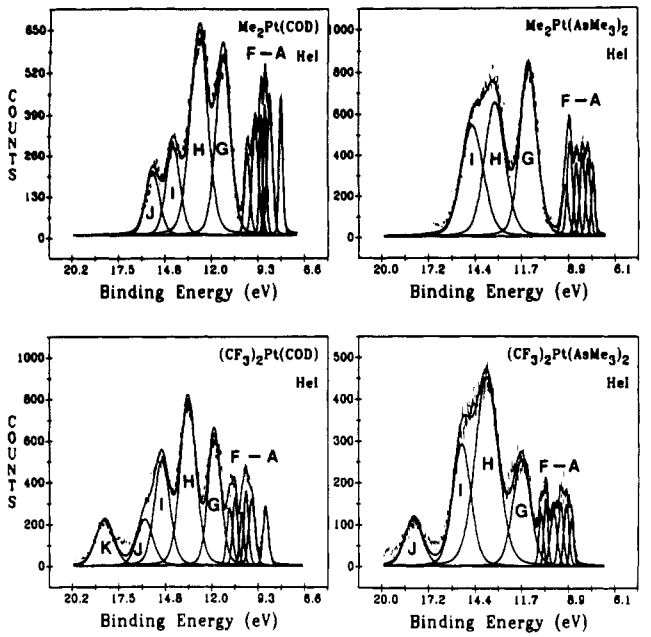

Figure 1. He I spectra of *cis*-$[PtR_2(AsMe_3)_2]$ and $[PtR_2(COD)]$ (R = CH_3 and CF_3).

atomic α's was employed, the weight being the number of the valence electrons in the neutral atoms.[17] Overlapping sphere radii were used.[18,19] An l_{max} of 3 was used around outer-sphere region and Pt whereas l_{max} values of 2, 1, and 0 were used around P, C and F, and H atoms, respectively. The geometries were based on the X-ray data of similar compounds, and the compounds were assumed to have C_{2v} symmetry.[20]

Results and Discussion

General Features of the Spectra. Some representative spectra are shown in Figure 1, along with the corresponding spectra for the dimethylplatinum(II) complexes for comparison. Further spectra of the complexes are given in Figures 2 and 3. By analogy, it is convenient to discuss the regions of the spectra in the ionization range >11.5 eV (bands labeled G–J(K)) and <11.5 eV (bands labeled A–F) separately. It is interesting to note that the ionization bands in the range >11.5 eV are less shifted than those in the range <11.5 eV upon replacement of CH_3 by CF_3. This leads to a smaller energy separation between the two regions of the spectra when compared to the dimethylplatinum complexes, as indicated by the separation of the band G from the band F in Figure 1. As for the dimethylplatinum compounds,[12] bands A–F are due to the contributions from mostly Pt and Pt–CF_3 orbitals. In the range >11.5 eV, the spectra contain broad envelopes, which are fitted to the minimum number of bands, but which probably contain contributions from ionizations of many ligand-based MO's as well as the lowest energy (largest ionization energy) metal–ligand MO's. The highest IE band at ~18 eV is absent in the spectra of the dimethylplatinum(II) complexes and thus is assigned to ionizations of C–F σ orbitals.[21] The fluorine p lone pairs, which ionize at ~14 eV, contribute to, for example, band H in the L = $AsMe_3$ complex and band I in the L_2 = COD complex, as

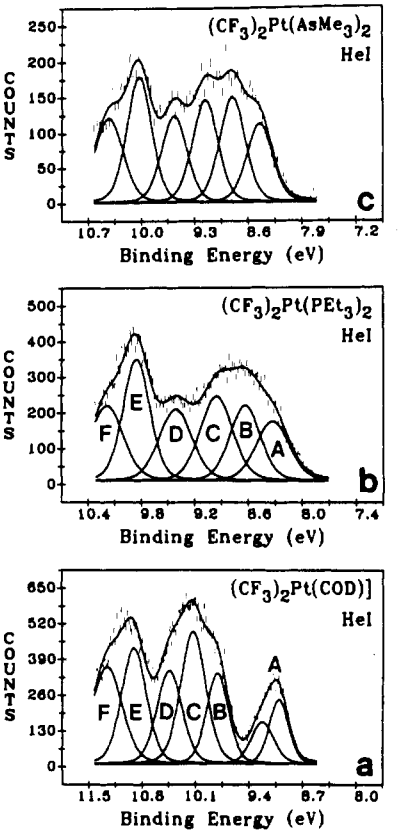

Figure 2. He I spectra of $[Pt(CF_3)_2(COD)]$ (a), *cis*-$[Pt(CF_3)_2(PEt_3)_2]$ (b), and *cis*-$[Pt(CF_3)_2(AsMe_3)_2]$ (c) (expanded first part only).

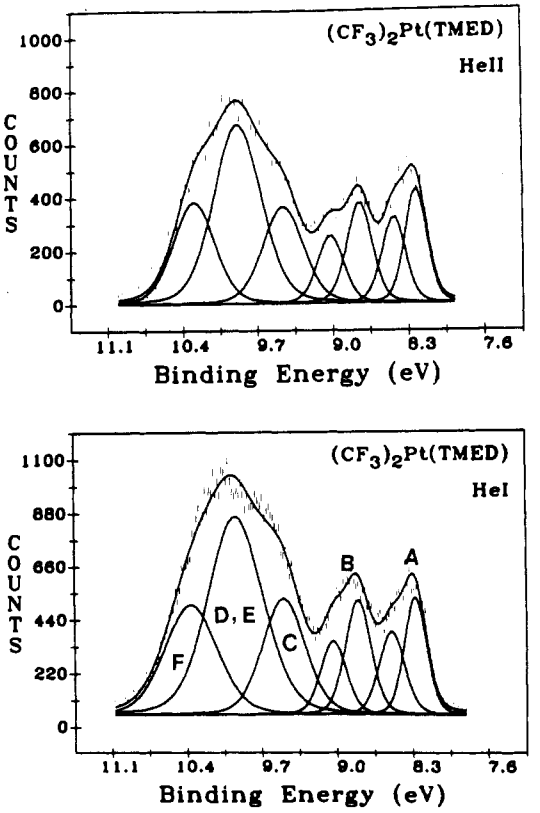

Figure 3. He I and He II spectra of $[Pt(CF_3)_2(TMED)]$ (expanded first part only).

indicated by the relative area increases from the dimethylplatinum(II) to the bis(trifluoromethyl)platinum(II) compounds (Figure 1), as well as by the higher He II/He I intensity ratios than those of the other bands in this region.[21-23] Band G at least

(17) Exchange factors for extramolecular and intersphere regions: $Pt(CF_3)_2(PH_3)_2$, 0.73550; $Pt(CF_3)_2(C_2H_4)_2$, 0.74213; $Pt(CF_3)_2$, 0.73287.
(18) Norman, J. G., Jr. *J. Chem. Phys.* **1974**, *61*, 4630. Norman, J. G., Jr. *Mol. Phys.* **1976**, *31*, 1191.
(19) Atomic and outer-sphere radii (bohrs) are as follows. $Pt(CF_3)_2(PH_3)_2$: outer, 7.0803; Pt, 2.6577; C, 1.6794; P, 2.3080; F, 1.7048; H, 1.4040. $Pt(CF_3)_2(C_2H_4)_2$: outer, 7.0200; Pt, 2.6577; C, 1.6794; F, 1.6802; H, 1.2100. $Pt(CF_3)_2$: outer, 6.4698; Pt, 2.6577; C, 1.6794; F, 1.6802.
(20) Pt–C = 2.058 Å and ∠C–Pt–C = 88.0° (Manojlovic-Muir, L.; Muir, K. W.; Solomun, T.; Meek, D. W.; Pertson, J. L. *J. Organomet. Chem.* **1978**, *146*, c26). C–F = 1.340 Å and ∠C–Pt–C = 88° *146*, c26). C–F = 1.340 Å and ∠F–C–F = 109.5° (Hall, M. B.; Fenske, R. F. *Inorg. Chem.* **1972**, *11*, 768). Other geometric parameters are the same as those in the corresponding dimethylplatinum(II) compounds (see ref 12).
(21) Drake, J. E.; Eujen, R.; Gorzelska, K. *Inorg. Chem.* **1982**, *21*, 1784.

Table I. Ionization Energies (eV), He II/He I Intensity Ratios, and Assignments of the Bands for *cis*-$[Pt(CF_3)_2L_2]$ (L_2 = COD, TMED; L = PEt_3, $AsMe_3$)

	COD		TMED			PEt_3		$AsMe_3$	
band	IE	He II/He I	IE	He II/He I	assgnt	IE	He II/He I	IE	assgnt
A	9.00	1.00	8.26	1.00	$4a_1$	8.33	1.00	8.42	$4a_1$
	9.20		8.45						
B	9.80	0.87	8.80	0.87	$2b_2$	8.63	1.04	8.78	$2b_2$
			9.00						
C	10.12	0.86	9.49	0.85	$3a_1$	8.95	0.97	9.15	$3a_1$
D	10.43	0.82	9.96	0.96	$1a_2$	9.41	0.95	9.56	$1b_1$
E	10.90	0.93	9.96	0.96	$1b_1$	9.85	1.02	10.03	$2a_1$
F	11.26	0.96	10.41	1.04	$2a_1$	10.19	1.01	10.43	$1a_2$

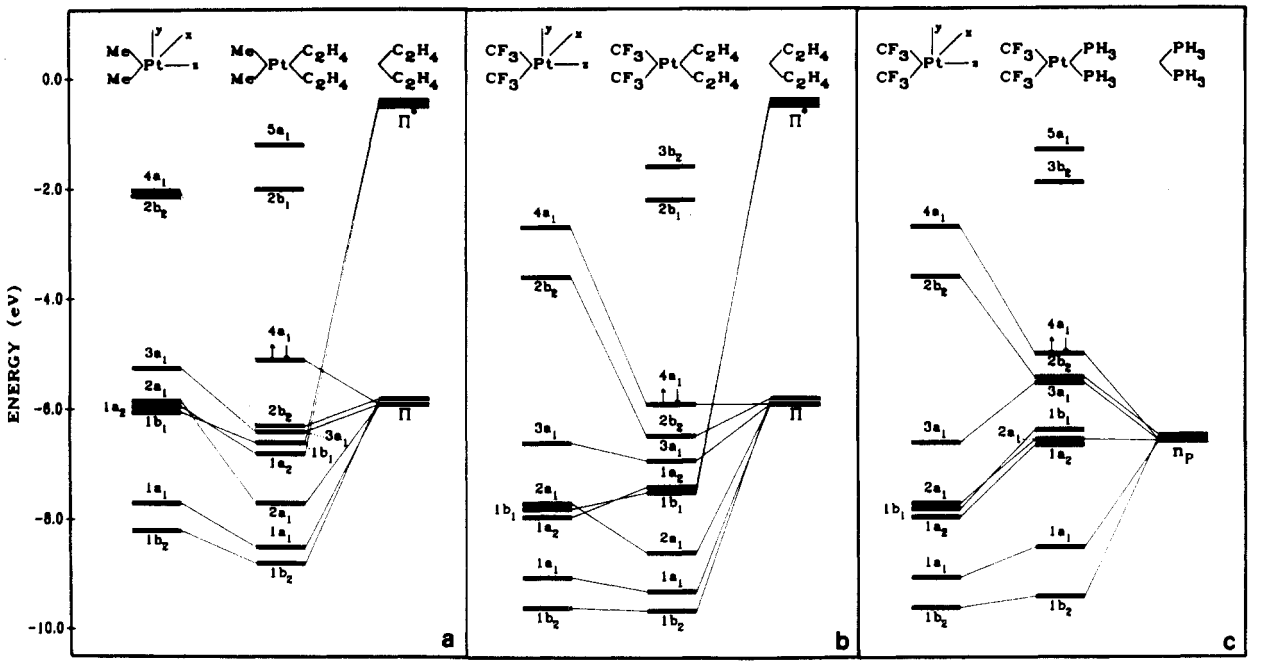

Figure 4. Orbital correlation diagrams for *cis*-$[PtMe_2(C_2H_4)_2]$ (a), *cis*-$[Pt(CF_3)_2(C_2H_4)_2]$ (b), and *cis*-$[Pt(CF_3)_2(PH_3)_2]$ (c).

partially arises from the ionizations of As–C orbitals, since the ionization energy is approximately the same as that of As–C orbitals in the free ligand $AsMe_3$ and remains almost unchanged in both *cis*-$[PtMe_2(AsMe_3)_2]$ and *cis*-$[Pt(CF_3)_2(AsMe_3)_2]$.[24] The He II/He I intensity ratios are much lower for the non-fluorine-containing bands in this high-IE region than for the bands at IE's <11.5 eV, as expected for ligand-based ionizations. This region at >11.5 eV will not be discussed further.

In the region <11.5 eV, the spectra are not resolved as well as those of the dimethylplatinum(II) complexes due to the broader inherent line width,[25] but typically six bands are satisfactorily fitted except for $[Pt(CF_3)_2(TMED)]$, in which two of the bands appear to be degenerate. The spectra are shown in Figures 2 and 3, and the data are given in Table I. There are three important features in the spectra of this region. First, the first band labeled A in $[Pt(CF_3)_2L_2]$ (L_2 = COD, TMED) clearly has an asymmetric shape although it is not resolved as well as the same band in $[PtMe_2L_2]$ (L_2 = COD, TMED). Thus, this band was fitted to two peaks with separations of 0.20 ± 0.04 eV in $[Pt(CF_3)_2(COD)]$ and of 0.19 ± 0.04 eV in $[Pt(CF_3)_2(TMED)]$. The band B in $[Pt(CF_3)_2(TMED)]$ was also fitted to two peaks due to its asymmetric shape with a separation of 0.20 ± 0.04 eV. These splittings are similar to, but larger than, the splittings in the corresponding dimethylplatinum complexes and are probably vibrational in origin.[12] Second, the perfluoromethyl effect causes a stabilization of all orbitals by ~1 eV when compared with the corresponding methylplatinum complexes. Finally, the six bands often give He II/He I band area ratios very similar to those for the dimethylplatinum compounds.

Since a platinum(II) complex should have four filled 5d orbitals, two of the six bands must be due to the metal–ligand σ MO's. For transition-metal complexes it is often possible to distinguish between d orbitals and σ orbitals by comparing the band intensities in the He I and He II spectra, since d orbitals typically have a greater relative photoionization cross section for He II radiation.[26,27] However, as the data in Table I indicate, the six bands display very similar He II/He I band area ratios and so this empirical method is not useful for these bis(trifluoromethyl)-platinum(II) complexes or for the previously studied Pt complexes.[12,28] Therefore, the spectra will be assigned by comparison

(22) Coleman, A. W.; Green, J. C.; Hayes, A. J.; Seddon, E. A.; Lloyd, D. R.; Nowa, Y. *J. Chem. Soc., Dalton Trans.* **1979**, 1057.
(23) Cauletti, C.; Clark, J. P.; Green, J. C.; Jackson, S. E.; Fragala, I. L.; Ciliberto, E.; Coleman, A. W. *J. Electron Spectrosc. Relat. Phenom.* **1980**, *18*, 61.
(24) Elbel, S.; Bergmann, H.; Enblin, W. *J. Chem. Soc., Faraday Trans. 2* **1974**, *70*, 555.
(25) Bristow, D. J.; Bancroft, G. M. *J. Am. Chem. Soc.* **1983**, *105*, 5634. Yates, B. W.; Tan, K. H.; Bancroft, G. M.; Coatsworth, L. L.; Tse, J. S. *J. Chem. Phys.* **1985**, *83*, 4906. Yates, B. W.; Tan, K. H.; Bancroft, G. M.; Tse. J. S. *J. Chem. Phys.* **1986**, *85*, 3840 and references therein.
(26) Louwen, J. N.; Hengenlmolen, R.; Grove, D. M.; Oskam, Ad. *Organometallics* **1984**, *3*, 908. Louwen, J. N.; Grove, D. M.; Ubbels, H. J. C.; Stufkens, D. J.; Oskam, Ad. *Z. Naturforsch., B* **1983**, *38*, 1657. Oskam, Ad.; Stufkens, D. J.; Louwen, J. N. *J. Mol. Struct.* **1986**, *142*, 347. Bella, S. D.; Fragala, I.; Granozzi, G. *Inorg. Chem.* **1986**, *25*, 3977. Granozzi, G.; Zangrande, G.; Bonivento, M.; Michelon, G. *Inorg. Chim. Acta* **1983**, *77*, L229.
(27) Bancroft, G. M.; Chan, T.; Puddephatt, R. J.; Tse, T. S. *Inorg. Chem.* **1982**, *21*, 2946. Bancroft, G. M.; Chan, T.; Puddephatt, R. J. *Inorg. Chem.* **1983**, *22*, 2133.
(28) Yang, D. S.; Bancroft, G. M.; Puddephatt, R. J.; Bursten, B. E.; McKee, S. O. *Inorg. Chem.* **1989**, *28*, 872.

Table II. MS-Xα Results for *cis*-[$Pt(CF_3)_2$] Upper Valence Orbitals

orbital[a]	Xα orbital energy, eV	charge distribution,[b] %				
		Pt	C	F	inter	outer
$4a_1$	2.71	9 s, 9 p_z, 5 d_{z^2}	2 s, 7 p	2 p	46	20
$2b_2$	3.62	11 p_y, 30 d_{yz}	7 s, 19 p	10 p	20	3
$3a_1$	6.56	16 s, 1 p_z, 33 $d_{x^2-y^2}$	3 s, 11 p	14 p	21	1
$2a_1$	7.79	89d_{z^2}		3 p	8	
$1b_1$	7.84	90 d_{xz}		2 p	8	
$1a_2$	7.93	89 d_{xy}		2 p	9	
$1a_1$	9.07	2 s, 1 p_z, 50 $d_{x^2-y^2}$	2 s, 12 p	25 p	8	
$1b_2$	9.62	46 d_{yz}	2 s, 10 p	34 p	7	1

[a] $3a_1$ is HOMO. [b] For the Pt contributions, the % contribution followed by the orbital is given. The partial p or d orbital is not given by the calculation directly, and the assignment of, for example, an a_1 orbital to mostly d_{z^2} or $d_{x^2-y^2}$ is based on the MO contours. These assignments are therefore not certain. This explanation is followed in the other tables.

Table III. MS-Xα Results for *cis*-[$Pt(CF_3)_2(C_2H_4)_2$] Upper Valence Orbitals

orbital	energy, eV		charge distribution, %						
	Xα orbital	trans state	Pt	C[a]	C[b]	F	H	inter	outer
$4a_1$	5.89	8.36	4 p_z, 17 d_{z^2}, 1 f	2 s, 7 p	39 p	4 p		25	
$2b_2$	6.49	8.92	6 p_y, 1 d_{yz}	2 s, 5 p	49 p	7 p		29	1
$3a_1$	6.89	9.38	14 s, 2 p_z, 36 $d_{x^2-y^2}$	2 s, 8 p	6 p	12 p	1	18	1
$1a_2$	7.46	10.02	44 d_{xy}		1 s, 23 p	1 p	24	7	
$1b_1$	7.51	10.13	75 d_{xz}		6 p	2 p	9	8	
$2a_1$	8.59	11.18	2 s, 70 d_{z^2}		11 p	3 p		14	
$1a_1$	9.29	11.79	1 s, 2 p_z, 46 $d_{x^2-y^2}$	2 s, 11 p	6 p	24 p	1	5	2
$1b_2$	9.61	12.06	35 d_{yz}	2 s, 11 p	1 s, 11 p	1 s, 25 p	6	5	2

[a] Carbon in CF_3. [b] Carbon in C_2H_4.

with the theoretical predictions based on calculations on the model compounds *cis*-[$Pt(CF_3)_2(C_2H_4)_2$] and *cis*-[$Pt(CF_3)_2(PH_3)_2$] and by comparison with the spectra of the corresponding dimethylplatinum(II) complexes,[12] since the theoretical calculations predict that the perfluoromethyl effect does not change the orbital sequence found for the methyl compounds.

Molecular Orbital Calculations. (a) Complex *cis*-[$Pt(CF_3)_2(C_2H_4)_2$]. In order to draw up an energy correlation diagram, the molecule *cis*-[$Pt(CF_3)_2(C_2H_4)_2$] has been considered to be formed by combination of the fragments of *cis*-[$Pt(CF_3)_2$] and $(C_2H_4)_2$, and calculations have been carried out for each species. In the correlation diagram of Figure 4b, only the interactions between the $Pt(CF_3)_2$ orbitals and the π and π^* orbitals of the ligand C_2H_4 are presented for the sake of simplicity. Our analysis will begin with a consideration of the fragment $Pt(CF_3)_2$ and a comparison with the fragment $PtMe_2$, which has been calculated before[12] and is presented in Figure 4a.

The results of the MS-Xα calculation for the *cis*-[$Pt(CF_3)_2$] fragment are given in Table II and in Figure 4b and in many respect are similar to those for *cis*-[$PtMe_2$].[12] Thus, there are two Pt-C σ levels ($1b_2$ and $1a_1$) below four orbitals that have mostly platinum 5d character ($2a_1$, $1b_1$, $1a_2$, and $3a_1$). The orbital $1b_2$ is formed by overlap of the $5d_{yz}$ orbital on platinum with the unsymmetrical combination of CF_3 σ orbitals, but there is also considerable fluorine 2p character in this MO (Table II). Similarly, the $1a_1$ orbital is formed from the 6s and $5d_{x^2-y^2}$ and $5d_{z^2}$ orbitals on platinum combining with the symmetric combination of CF_3 σ orbitals, and again there is much fluorine 2p character. Of the platinum 5d levels, three have 89-90% d character and are assigned as $1a_2$ ($5d_{xy}$), $1b_1$ ($5d_{xz}$), and $2a_1$ ($5d_{z^2}$), while the HOMO $3a_1$ has only 33% platinum 5d character ($5d_{x^2-y^2}$), with some 6s character and cleary some σ^* character. The virtual orbitals $2b_2$ and $4a_1$ are the σ^*-antibonding levels, corresponding to the bonding levels $1b_2$ and $1a_1$, respectively.

It is interesting to note that the nonbonding platinum 5d orbitals $1a_2$, $1b_1$, and $2a_1$ are calculated to be about 1.9 eV lower in energy than for the dimethylplatinum fragment, while the Pt-C σ orbitals $1b_2$ and $1a_1$ are lower in energy compared to the $PtMe_2$ fragment by only about 1.4 eV. The general stabilization is clearly due to the inductive effects of the electronegative fluorine atoms, but the predicted smaller stabilization of the σ orbitals is probably a result of the poor energy matching and overlap between the Pt 5d orbitals and the CF_3 σ orbitals, since the CF_3 fragment is more electronegative than that of CH_3.

In considering the interaction of the *cis*-[$Pt(CF_3)_2$] fragment with ethylene, the orbitals of interest of the *cis*-$(C_2H_4)_2$ ligands are the π orbitals ($a_1 + b_2$) and the π^* orbitals ($a_2 + b_1$) arising from the C=C bonds. The energies as calculated are shown in Figure 4b. It is clear from the resulting correlation diagram and from the orbital characters given in Table III that the two σ orbitals ($1b_2 + 1a_1$) of the fragment $Pt(CF_3)_2$ are perturbed only slightly and hence the molecular orbitals labeled $1a_1$ and $1b_2$ retain their largely Pt-CF_3 σ character. As for the fragment $PtMe_2$, the two empty orbitals ($4a_1 + 2b_2$) of the fragment $Pt(CF_3)_2$ mix strongly with the π electrons of the ethylene ligand, and this interaction produces molecular orbitals $4a_1$ and $2b_2$ of much lower energy. The orbital $2b_2$ of *cis*-[$Pt(CF_3)_2(C_2H_4)_2$] is calculated to have mostly C=C π character (Table III), and it has the smallest energy shift ($\sim$0.15 eV) compared to the orbital $2b_2$ in *cis*-[$PtMe_2(C_2H_4)_2$], whereas the other orbitals in the lower ionization energy region are stabilized by 0.70 $\pm$ 0.20 eV, compared to the corresponding orbitals in *cis*-[$PtMe_2(C_2H_4)_2$]. The HOMO is $4a_1$, which has mainly Pt-C_2H_4 σ character along with some Pt-CF_3 σ^* character, as indicated by the contour diagram in Figure 5. The contours were plotted on the molecular plane with the CF_3 groups on the upper side and the C_2H_4 groups on the down side with respect to the platinum atom. It is very obvious from the contours in Figure 5 that the contribution of the CF_3 groups to each MO is always C-F σ^* character instead of the carbon 2p orbital alone.

As for the middle four levels ($3a_1 + 2a_1 + 1b_1 + 1a_2$) of the fragment $Pt(CF_3)_2$, it can be seen from the correlation diagram that the $2a_1$ orbital and, to a lesser extent, the $3a_1$ orbital are stabilized by the symmetric mixing with the a_1 combination of C_2H_4 π orbitals. On this basis the $3a_1$ orbital can be considered having largely nonbonding Pt 5d character though it is involved in σ bonding to C_2H_4 and σ^* antibonding to CF_3. The orbitals $1a_2$ and $1b_1$ of the fragment $Pt(CF_3)_2$ are predicted to be destabilized on formation of *cis*-[$Pt(CF_3)_2(C_2H_4)_2$], which is perhaps surprising, since both the $1b_1$ and $1a_2$ orbitals are expected to be stabilized by back-bonding to the C_2H_4 π^* orbitals. The back-bonding is probably weaker than in the complex *cis*-[$PtMe_2(C_2H_4)_2$], for which the orbitals $1b_1$ and $1a_2$ of the fragment $PtMe_2$ were calculated to be stabilized.[12] Indeed, the calculations for

Table IV. MS-Xα Results for *cis*-$[Pt(CF_3)_2(PH_3)_2]$ Upper Valence Orbitals

orbital	energy, eV: Xα orbital	energy, eV: trans state	charge distribution, %: Pt	C	P	F	H	inter	outer
$4a_1$	5.13	7.65	10 s, 6 p_z, 25 d_{z^2}	5 s, 17 p	3 p	17 p		16	1
$2b_2$	5.56	8.05	13 p_y, 3 d_{yz}	5 s, 17 p	3 s, 25 p	15 p	4	15	
$3a_1$	5.63	8.10	8 s, 7 p_z, 23 $d_{x^2-y^2}$	1 s, 5 p	1 s, 27 p	2 p	5	19	2
$1b_1$	6.38	9.11	86 d_{xz}		2 d	2 p	3	7	
$2a_1$	6.51	9.22	79 d_{z^2}	1 p	2 p, 3 d	3 p	5	7	
$1a_2$	6.55	9.27	83 d_{xy}		3 d	1 p	4	9	
$1a_1$	8.53	11.08	6 s, 36 $d_{x^2-y^2}$	1 s, 4 p	18 p, 2 d	20 p	7	4	2
$1b_2$	9.40	11.97	41 d_{yz}	1 s, 4 p	19 p, 2 d	20 p	10	3	

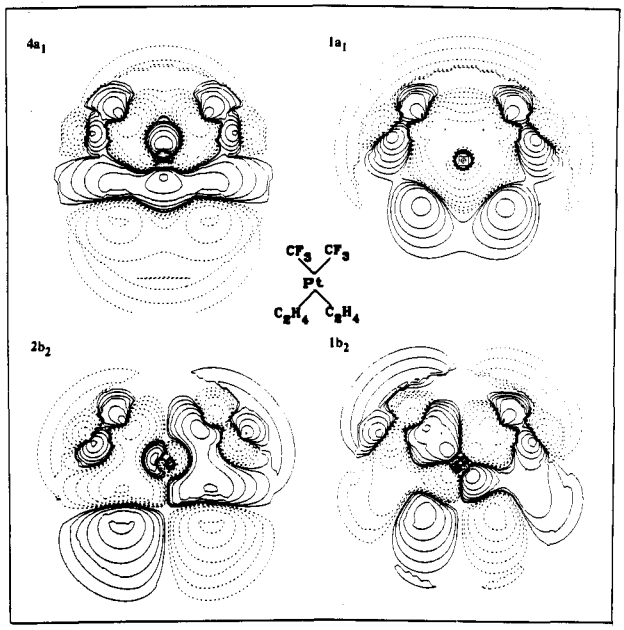

Figure 5. Contour maps of $1a_1$, $1b_2$, $2b_2$, and $4a_1$ orbitals for *cis*-$[Pt(CF_3)_2(C_2H_4)_2]$. The contours are plotted at values ±0.002, ±0.0047, ±0.0094, ±0.0188, ±0.0375, and ±0.15, starting from the outermost region.

cis-$[Pt(CF_3)_2(C_2H_4)_2]$ show some H character in the orbitals $1a_2$ and $1b_1$ consistent with C_2H_4 acting as a weak π donor as well as a σ donor to platinum.

(b) Complex *cis*-$[Pt(CF_3)_2(PH_3)_2]$. The results for this complex are similar to those for *cis*-$[Pt(CF_3)_2(C_2H_4)_2]$ and so are treated more briefly (Figure 4c and Table IV). The calculations on the free ligand PH_3 indicate that the lone-pair orbitals of symmetry $a_1 + b_2$ have mostly p character.[12] The empty orbital at −0.38 eV has major contributions from the outer-sphere region and probably is a Rydberg orbital. It is therefore not shown in the correlation diagram (Figure 4c).

Compared to the case for *cis*-$(C_2H_4)_2$, the lone pair orbitals of the two PH_3 interact more strongly with the $1b_2$ and $1a_1$ levels of the fragment $Pt(CF_3)_2$, leading to both CF_3 and PH_3 having comparable contributions to the MO's $1b_2$ and $1a_1$. In contrast, the lone-pair PH_3 orbitals interact less strongly with the $4a_1$ and $2b_2$ levels, resulting in the $4a_1$ MO having largely Pt–CF_3 character and the $2b_2$ MO being fairly evenly distributed among the Pt, CF_3, and PH_3 groups (Table IV). In addition, the orbitals $3a_1$, $2a_1$, $1a_2$, and $1b_1$, which were identified earlier as having mostly Pt 5d character, are less strongly perturbed by additional mixing with PH_3 compared with C_2H_4. In contrast to the dimethylplatinum analogue, it is interesting to note that most of the occupied orbitals of the fragment $Pt(CF_3)_2$ increase in energy by taking on *cis*-$(PH_3)_2$. This is a reflection of the significant charge transfer to the fragment $Pt(CF_3)_2$ from the ligand PH_3.

Compared to the case for *cis*-$[PtMe_2(PH_3)_2]$, the orbital interactions between the fragments $PtMe_2$ and $(PH_3)_2$ are rather similar to those between the fragments $Pt(CF_3)_2$ and $(PH_3)_2$. But more charge transfer to $Pt(CF_3)_2$ from PH_3 is implied by the relative energy shifts of the $Pt(CF_3)_2$ and $PtMe_2$ orbitals, especially for the nonbonding Pt 5d orbitals, upon PH_3 attachment.

Spectral Assignment and Interpretation. (a) Complex $[Pt(CF_3)_2(COD)]$. The low-IE region of the fitted spectrum is given in Figure 2a. Five of the six bands (B–F) could be fitted to single Lorentzian–Gaussian shapes. Band A is clearly asymmetric and thus was fitted to two peaks with a separation of 0.20 ± 0.04 eV (~1600 ± 320 cm^{-1}), comparable to the separation of 0.17 ± 0.02 eV (~1400 ± 160 cm^{-1}) of the band A in $[PtMe_2(COD)]$, which was assigned due to vibrational splitting of the C=C bond. Therefore, this splitting is also assigned to vibration coupling and indicates that the HOMO has substantial platinum–alkene bonding character, as is predicted by the MS-Xα calculation on the model compound *cis*-$[Pt(CF_3)_2(C_2H_4)_2]$. The relatively large error in energy is due to the poor resolution of the vibrational splitting in this band. Band B is assigned to the orbital $2b_2$ (Figure 4a) on the basis of the MS-Xα calculation on the model *cis*-$[Pt(CF_3)_2(C_2H_4)_2]$. Vibrational splitting of this band would be expected, since much C=C ligand character in this MO was predicted theoretically (Table III), but was not resolved because of overlap with band C (Figure 2a). It is then natural to assign the next four bands (C–F) to ionizations of four orbitals with mostly Pt 5d character. There is no experimental evidence to aid assignment of each band to a specific d orbital, and so the assignments in Table I are based on the MS-Xα predictions only. These are therefore tentative assignments only.

Consider next the energy shift of the alkene π orbitals on coordination. Free COD shows one π ionization band at 9.06 eV,[29] while the σ orbitals in *cis*-$[Pt(CF_3)_2(C_2H_4)_2]$ having the most character of the alkene π orbitals are $4a_1$ and $2b_2$, which appear in the spectrum at 9.00/9.20 eV (vibrational coupling) and 9.80 eV, respectively. This indicates that the π orbitals are stabilized on coordination, suggesting that the alkene σ donation is more important than its π acceptance, in agreement with the theoretical prediction of Figure 4b.

(b) Complex $[Pt(CF_3)_2(TMED)]$. The He I and He II spectra in the low-IE region are displayed in Figure 3, and they are very similar to the spectra of $[PtMe_2(TMED)]$. By comparison, bands A and B are assigned to platinum–ligand σ MO's and bands C–F to four MO's having mostly Pt 5d character, as given in Table I.

In $[PtMe_2(TMED)]$, band A was split into two peaks with a separation of 0.13 ± 0.02 eV and this splitting was assigned to the C–N vibrational coupling. The C–N vibrational splitting of the band B was also expected on the basis of an MS-Xα calculation on *cis*-$[PtMe_2(NH_3)_2]$ but was not resolved because of its closeness to band C. In the complex $[Pt(CF_3)_2(TMED)]$, bands A and B are both asymmetric and they were both fitted as two peaks with separations of 0.19 ± 0.04 and 0.20 ± 0.04 eV, respectively. These splittings could be assigned to the C–N vibrational coupling although the separations here are somewhat larger than that observed in $[PtMe_2(TMED)]$. There are two reasons causing the larger separations. One is the relatively large error in the energy determinations due to the poor resolution of the vibrational splittings of the bands A and B. The theoretical calculation has predicted that the first two MO's with higher energies in *cis*-$[PtMe_2(NH_3)_2]$ contain a large contribution from

(29) Batich, C.; Ermer, O.; Heilbronner, E. *J. Electron Spectrosc. Relat. Phenom.* **1973**, *1*, 333.

the methyl groups. Although we did not perform the calculation for *cis*-$[Pt(CF_3)_2(NH_3)_2]$, the first two MO's are expected to have significant CF_3 character, since CF_3 substitution does not change the general MO sequence, as calculated for phosphine and ethylene compounds. Therefore, the other possible reason may be due to both C-N and C-F stretching vibrational modes of the same symmetry being excited upon molecular ionization. In this case, frequency comparisons between molecule and ion become meaningless, as pointed out by Eland.[30] The fourth band labelled D,E has about twice the area of the other bands and is thus assigned as due to two almost degenerate MO's. Because TMED has no π-acceptor properties, the platinum d_π orbitals, d_{xz} ($1b_1$) and d_{xy} ($1a_2$), are expected to be close in energy. The fourth band is therefore assigned to these platinum d_π orbitals. The assignments for the other bands are made in a way similar to that for $[PtMe_2(TMED)]$.[12]

(c) Complexes *cis*-$[Pt(CF_3)_2(PEt_3)_2]$ and *cis*-$[Pt(CF_3)_2(AsMe_3)_2]$. The low-IE regions of the spectra for these complexes are similar, as shown in Figure 2b,c. The spectra are less resolved than those for the complexes discussed above, but the spectra were fitted most satisfactorily with six bands. In no case does band A or B show resolved vibrational structure, in contrast to the observations for the COD and TMED complexes. Such splitting may not be expected, since the characteristic ν(PC) and ν(AsC) frequencies are too low to give resolved fine structure.[31] The bands A and B (or bands B and C) are also close in energy and fairly broad, which would make vibrational couplings difficult to resolve.

The spectra give very similar He II/He I intensity ratios (Table I), and ionization energies of all bands shift by a similar amount when compared to the corresponding methylplatinum complexes. Thus, it is again not possible to distinguish between the metal orbitals and the metal-ligand σ MO's on an experimental basis. Therefore, the spectral assignments given in Table I are based on the predictions of the MS-Xα calculations on *cis*-$[Pt(CF_3)_2(PH_3)_2]$ and are similar to those for the corresponding dimethylplatinum(II) complexes.

Pt-CF_3 Bonding and the CF_3 Ligand Effect. From the preceding discussions, at least two features of Pt-CF_3 bonding in these complexes can be summarized as follows: (a) There is considerable C-F antibonding character with significant carbon 2s character in the Pt-CF_3 bonds. In contrast, there is essentially only the carbon 2p lone-pair contribution to the σ-donor orbital of the methyl group in Pt-CH_3 bonding. (b) π interactions between filled d_π orbitals on platinum and σ^* orbitals of the perfluoromethyl group are very weak, as evidenced by the very small fluorine character present in the MO's $1b_1$ and $1a_2$. Since similar platinum 6s character is predicted in both Pt-CF_3 and Pt-CH_3 bonds by MS-Xα calculations, in agreement with their comparable NMR trans influence,[5,6] the observed Pt-C shortening (0.04-0.06 Å)[4,32] in bis(trifluoromethyl)platinum(II) complexes compared to dimethylplatinum(II) complexes could only be explained in terms of the different carbon 2s contributions. In forming a bond with platinum, the perfluoromethyl group will naturally approach closer than the methyl group to the Pt atom because of its greater carbon 2s contribution. This interpretation is in accord with Fenske-Hall calculations on $(CF_3)Mn(CO)_5$ and $(CH_3)Mn(CO)_5$.[11]

From this work, combined with our previous study on the corresponding dimethylplatinum(II) complexes, it can also be noted that the CF_3 substituent, R = CF_3, causes greater σ donation from the ligand L to platinum in the phosphine complex *cis*-$[PtR_2L_2]$ (Figure 4c) and less π back-donating from platinum to the ligand L as in the alkene complex (Figure 4b) compared to their derivatives with R = CH_3. The overall effect still results in more positive charge on platinum, as shown experimentally by the higher ionization energies of the Pt 5d orbitals when R = CF_3. The greater positive charge on platinum will naturally lead to the deactivation of the metal center toward oxidative addition, in agreement with the chemical observations. In addition, the higher ionization energies of the platinum 5d as well as σ orbitals account at least in part for the higher thermal stability of the perfluoromethyl complexes.

Conclusions

The UV photoelectron spectra of the *cis*-bis(trifluoromethyl)platinum(II) complexes can be assigned by comparison with the theoretical predictions based on calculations on the model compounds *cis*-$[Pt(CF_3)_2(C_2H_4)_2]$ and *cis*-$[Pt(CF_3)_2(PH_3)_2]$ and by comparison with the spectra of the corresponding dimethylplatinum(II) complexes. The first two ionization bands with low ionization energies are assigned to the platinum-ligand σ orbitals, followed by the essentially nonbonding platinum 5d orbitals. The nature of the Pt-CF_3 σ bonding can be discussed in terms of MS-Xα results. the CF_3 contribution to the Pt-CF_3 σ bonds arises from the C-F antibonding orbitals with considerable carbon 2s character, rather than pure carbon 2p character.

Acknowledgment. We are grateful to the NSERC for financial support.

(30) Eland, J. H. D. *Photoelectron Spectroscopy*, 2nd ed.; Butterworth & Co. Ltd.: London, 1984; p 138.
(31) Rao, C. N. R. *Chemical Applications of Infrared Spectroscopy*; Academic Press Inc. Ltd.: London, 1963.
(32) Wisner, J. M.; Bartczak, T. J.; Ibers, J. A. *Organometallics* **1986**, *5*, 2044.

Contribution from the Department of Chemistry and Biochemistry, University of California, Los Angeles, California 90024

The Emission Spectrum of Ruthenocene: Calculation of the Excited-State Distortions and the Spacings in the Repetitive Pattern

Gary J. Hollingsworth, Kyeong-Sook Kim Shin, and Jeffrey I. Zink*

Received September 29, 1989

The emission spectrum of crystalline ruthenocene at 10 K contains unusually well-resolved vibronic structure. The crystal spectrum consists of two long progressions in the 333-cm^{-1} metal-ring stretching mode that are separated from each other by 165 cm^{-1}. This separation is not present in the spectrum taken from an isooctane glass. Each of the progressions has the same lifetime but has different polarizations. Each of the peaks of the 333-cm^{-1} progression contains sidebands that are repeated throughout the spectrum. The spectrum is quantitatively calculated and interpreted by using the time-dependent theory of electronic spectroscopy. The repetition is interpreted in terms of beats in the recurrence of overlaps in the time domain. The complete spectrum is accurately calculated by using four displaced normal modes. The major displacement is along the metal-ring bond axis with minor contributions from ring tilting modes.

Introduction

The vibronic structure in the emission spectrum of ruthenocene, $Ru(\eta^5\text{-}C_5H_5)_2$, obtained at low temperature from single crystals contains three interesting features. The most striking feature is a repetitive pattern of clusters of bands consisting of a sharp peak and several weaker sidebands. This pattern is repeated over a

0020-1669/90/1329-2501$02.50/0